The basal layer in human squamous tumors harbors more UVA than UVB fingerprint mutations: A role for UVA in human skin carcinogenesis

Nita S. Agar*, Gary M. Halliday*†, Ross StC. Barnetson*, Honnavara N. Ananthaswamy‡, Mark Wheeler§, and Alexandra M. Jones*

*Dermatology Research Unit, Melanoma and Skin Cancer Research Institute, Sydney Cancer Centre, Royal Prince Alfred Hospital, University of Sydney, Sydney NSW 2006, Australia; ‡Department of Immunology, University of Texas M.D. Anderson Cancer Center, Houston, TX 77030; and §Millennium Institute, University of Sydney, Sydney NSW 2006, Australia

Communicated by Richard B. Setlow, Brookhaven National Laboratory, Upton, NY, February 17, 2004 (received for review December 11, 2003)

We hypothesized that a substantial portion of the mutagenic alterations produced in the basal layer of human skin by sunlight are induced by wavelengths in the UVA range. Using laser capture microdissection we examined separately basal and suprabasal keratinocytes from human skin squamous cell carcinomas and premalignant solar keratosis for both UVA- and UVB-induced adduct formation and signature mutations. We found that UVA fingerprint mutations were detectable in human skin squamous cell carcinomas and solar keratosis, mostly in the basal germinative layer, which contrasted with a predominantly suprabasal localization of UVB fingerprint mutations in these lesions. The epidermal layer bias was confirmed by immunohistochemical analyses with a superficial localization of cyclobutane thymine dimers contrasting with the localization of 8-hydroxy-2′-deoxyguanine adducts to the basal epithelial layers. If unrepaired, these adducts may lead to fixed genomic mutations. The basal location of UVA- rather than UVB-induced DNA damage suggests that longer-wavelength UVR is an important carcinogen in the stem cell compartment of the skin. Given the traditional emphasis on UVB, these results may have profound implications for future public health initiatives for skin cancer prevention.

Human epidermis is a heterogeneous tissue composed of several distinct layers. Based on incident energy, UVA induces less direct damage to DNA than UVB (1) and therefore has been considered far less carcinogenic. However, there are many unresolved issues regarding the relative carcinogenicity of UVA and UVB in human skin. UVA is ≈20-fold more intense than UVB in sunlight and is absorbed by different chromophores. *In vitro*, whole mouse and human epidermis attenuate UVB photons to a greater extent than those of UVA, with <10% of incident UVB radiation, but with >20% of UVA reaching the basal germinative layers (2). Initiation of skin tumors presumably requires penetration of UV photons to the dividing basal/stem cell layer for acute DNA damage to become fixed as heritable genomic mutations (3), and more UVA than UVB would be expected to reach this basal layer. Hence, UVA may make a larger contribution to human skin cancer than is generally assumed.

Despite estimates (4), neither the action spectra for skin cancer in humans nor the relative roles of UVA and UVB are known. UVB and UVA are both tumorigenic in mice (5). UVA rather than UVB mediates the dermal changes observed as photoaging, supporting a role for the increased penetrance of UVA. A large body of evidence now points to a role for UVA in skin carcinogenesis (6).

G:C → A:T transitions are considered UVB-induced when occurring at tandem dipyrimidine (Py-Py) sites or pyrimidine (Py) runs (7). The most common base change when DNA nucleotide excision repair-proficient Chinese hamster ovary cells, hemizygotic at *aprt*, were irradiated with UVA was A:T → C:G transversion (8), and UVA induces more sequence alterations at A:T base pairs and less G:C → A:T transitions than UVB and UVC in transfected *LacZ′* from partially transformed human cells (9). The high incidence of A:T → C:G transversions in cells exposed to solar-simulated UV versus those exposed to UVB established this base change as a potential molecular fingerprint to assess the genotoxicity of UVA (8). p53 is particularly valuable as a dosimeter of carcinogen exposure (10), because mutations often impart a "gain of oncogenic function," most skin squamous cell carcinomas (SCCs) and precancers in humans retain at least one mutant allele (11), and p53 mutational spectra have linked carcinogens to oncogenesis in several organ systems (10). The induction of premutagenic photoproducts are wavelength- and UVR dose-dependent, with cyclobutane Py dimers (CPDs) being predominantly induced by UVB wavelengths, whereas 8-hydroxy-2′-deoxyguanine (8-oxoG) remains one of the most common markers for evaluating UVA oxidative DNA damage in human skin cancer (12). We exploited the distinction between UVA and UVB DNA damage to search for both UVA and UVB UVR signature mutations and adduct formation, in particular A:T → C:G transversions in p53 in human SCCs and solar keratosis (SK). We report here *in vivo* evidence for the mutagenic role of UVA in the stem cell layer of human skin cancers.

Materials and Methods

Samples. Protocols were approved by the institutional human ethics committee, and 4-mm punch biopsies from the center of eight primary SCCs and eight excised SK were collected from 16 patients recruited through the Dermatology Clinic at Royal Prince Alfred Hospital (Camperdown, Australia). SK and SCCs were bisected: one half for histological diagnosis and the remaining half for use in the study. An independent pathologist classified the samples. Biopsies of normal, non-sun-exposed skin were used as controls from three age-matched patients. Samples were snap-frozen and stored at −70°C. Two serial 7-μm cryosections were microdissected as described (13) for mutational analysis, and the consecutive six serial sections were used for immunohistochemistry (IHC).

Microdissection. Cryosections on 3% glycerol-coated Superfrost slides were stained with hematoxylin/eosin. Dissection was carried out immediately by using a Pixcell II laser capture microdissection (LCM) system (Arcturus Engineering, Mountain View, CA). Seven areas were selected from each lesion,

Abbreviations: Py, pyrimidine; Py-Py, dipyrimidine; SCC, squamous cell carcinoma; CPD, cyclobutane Py dimer; 8-oxoG, 8-hydroxy-2′-deoxyguanine; SK, solar keratoses; IHC, immunohistochemistry; LCM, laser capture microdissection; ROS, reactive oxygen species.

†To whom correspondence should be addressed at: Division of Medicine (Dermatology), University of Sydney, Blackburn Building DO6, Sydney NSW 2006, Australia. E-mail: garyh@med.usyd.edu.au.

© 2004 by The National Academy of Sciences of the USA

www.pnas.org/cgi/doi/10.1073/pnas.0401141101

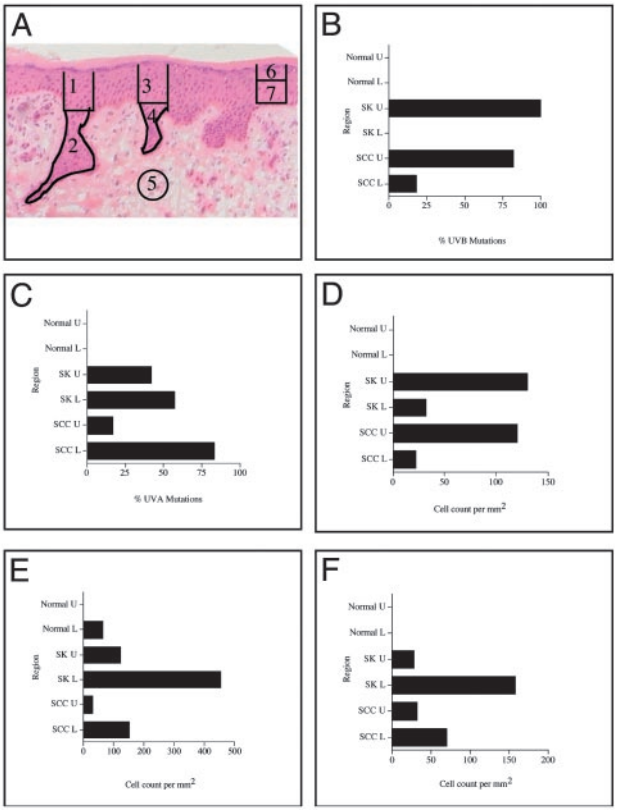

Fig. 1. (*A*) Regions sampled by LCM for mutational analysis in SK and SCCs. 1, uninflamed upper; 2, uninflamed lower; 3, inflamed upper; 4, inflamed lower; 5, stromal; 6, normal upper; 7, normal lower (note that only regions 6 and 7 sampled in normal control skin). (*B*) Distribution of UVB fingerprint mutations in SK, SCC, and normal skin. U, upper epidermal regions 1 and 3; L, lower epidermal regions 2 and 4. Normal U and Normal L are the mutations in the upper and lower epidermal regions, respectively, of control samples from non-sun-exposed skin. Region 6 and 7 (normal skin adjacent to the SK or SCC) data are not shown for these regions. (*C*) Distribution of UVA fingerprint mutations in SK, SCC, and normal skin. (*D*) Number of cells positive for CPDs as determined by IHC. The minimal number of CPD-positive cells in normal control skin is too small to be visualized. (*E*) Number of cells positive for 8-oxoG as determined by IHC. (*F*) Number of cells positive for p53 as determined by IHC.

including adjacent histologically normal skin as an internal control (Fig. 1*A*, regions 6 and 7). Two representative areas were sampled, one inflamed and one uninflamed; 20 stratum spinosum and granulosum cells (Fig. 1*A*, regions 1 and 3, respectively) and 20 stratum basale cells (Fig. 1*A*, regions 2 and 4, respectively) from each of two vertical rete pegs were sampled, with regions 1 and 3 being vertically above regions 2 and 4, respectively. Stromal cells at the base of the inflammatory peg (Fig. 1*A*, region 5) were sampled also. A total of 124 microdissected regions were collected.

p53 Mutational Analysis. Crude cell lysate (2 μl) from microdissected cells was used directly as a PCR DNA template; p53 exons 5–9 were amplified in all samples using the primers described (14). Each amplicon was purified by QIAquick (Qiagen, Valencia, CA) gel extraction before automated sequencing using an Applied Biosystems model 373A, and all amplicons and controls were sequenced in forward and reverse, to full length without cloning, in duplicate. Base misincorporation was limited by using Platinum Taq, and positive and negative control DNA fragments were sequenced accurately in every run. Sequence readouts were checked manually, downloaded to BIONAVIGATOR 3.0 for WebANGIS (Australian National Genomic Information Service, www.angis.org.au), and edited, and full exonic sequences including splice donor sites were aligned for comparison with *Homo sapiens* p53 (GenBank accession no. X54156) by using the nucleotide alignment program PRETTYBOX. A mutation was recorded only if detected in both strands and confirmed after repetition. All base changes were tabulated according to the sequence alteration, the sequence context (e.g., Py-Py site, 5′-GG-3′, and CpG), codon, amino acid change, the depth of the microdissected region from which the cell lysate was obtained, and the presence or absence of a dermal inflammatory infiltrate. Base changes were categorized as UVB fingerprints when G:C → A:T transitions occurred at Py-Py sites (CT, CC, TC) or Py runs, including tandem events such as C:C → T:T (or G:G → A:A); as UVA fingerprints when A:T → C:G transversion occurred (8); and as base changes not grouped as UVA fingerprints but potentially attributable to the effects of UVA either through type 1 electron-transfer mechanisms or major and minor type 2 mechanisms, being G:C → T:A and G:C → C:G transversion or G:C → A:T transition at non-Py-Py sites (15). A:T → G:C transitions and A:T → T:A transversions were grouped separately, being potentially attributable to both wavebands and additional mutagenic events. Although cytosine methylation significantly increases the yield of CPDs at CpG sites post-UVB irradiation (16), all CpG sites in human p53 are methylated and potentially affected by endogenous mutagenic events; therefore, G:C → A:T transition at CpG sites were grouped separately, not with UVB fingerprints.

Characterization of Dermal Inflammatory Infiltrate. To exclude the possible confounding effects of endogenous reactive oxygen species (ROS) production on base changes that otherwise would be attributable to the effects of UVA, one rete peg of the lesion was always adjacent to a more dense inflammatory infiltrate than the other area, and dermal stromal cells were sampled. We characterized the inflammatory cell type, cell number, depth of infiltrate, and endogenous H_2O_2 production in these regions. Both mutational and adduct data were compared between the areas with different degrees of inflammation.

IHC. Immunostaining was on 7-μm frozen sections using the streptavidin-biotin system, with alkaline phosphatase as the substrate and new fuchsin as the chromogen (17). Positive cells were quantified under light microscopy, with depth calculation performed by using a 0.0625-mm^2 grid. The following antibodies along with their isotype controls (which were used in equivalent protein concentrations to the antibody) were used: anti-thymine dimer H3 clone 4F6 (Affitech, Oslo) (18), isotype monoclonal $IgG_{1\lambda}$; anti-8-oxoG (Trevigen, Gaithersburg, MD) (19), isotype monoclonal IgG_1; mouse anti-human p53 clone D07 (DAKO) (20), isotype monoclonal IgG_{2b}; and mouse anti-human Mac 387 (DAKO), isotype monoclonal IgG_1. Diaminobenzidine alone without antibody was used to detect cells producing H_2O_2 (21).

Statistical Analysis. Immunohistochemical data were analyzed with unpaired Student's *t* tests. Depth analysis was performed by χ^2 tests with mutations stratified according to depth as either $\leq$0.4 mm or >0.4 mm from the surface of the stratum corneum.

Results

A summary of mutational data are given in Tables 1–4. Mutated bases are underlined in the text.

UVB Fingerprints (G:C → A:T Transitions at Py-Py Sites) Were Located in Keratinocytes in the Stratum Granulosum in SCCs and SK. Of the 18 G:C → A:T transitions in keratinocytes, 16 were in the superficial epithelial layers. In SK, seven were in the stratum granulosum and 0 were in the basal layer; in SCCs, nine were in the

Table 1. Types of mutations detected in exons 5–9 p53 in the stratum granulosum of human SK

Base change (total no.)	Coding strand	Codon p53	Sequence	AA change*	Lesion/ region†
UVA fingerprints					
AT → CG (3)	T → G	130	ccTc‡	**Leu → Arg**	SK1,1
	T → G	264	cTac‡	**Leu → Arg**	SK3,6
	A → C	198	gaAg‡	**Glu → Asp**	SK5,3
UVB fingerprints	C → T	145	gCtgt‡	Leu → Leu	SK1,6
GC → AT (7)	C → T	230	acCa‡§	Thr → Thr	SK3,1
	C → T	**278**	cCtg‡§	**Pro → Leu**	SK2,3
	C → T	252	ctCa‡	Leu → Leu	SK3,3
	C → T	250	ccCa‡§	Pro → Pro	SK4,3
	C → T	289	ctCc‡	Leu → Leu	SK5,6
	C → T	264	tCtag‡	Leu → Leu	SK8,3
ROS¶					
GC → TA (1)	C → A	252	ctCa‡	Leu → Leu	SK4,3
GC → CG (5)	G → C	282	cgGc‡	Arg → Arg	SK2,3
	C → G	289	ctCc‡	Leu → Leu	SK5,1
	C → G	253	acCa‡§	Thr → Thr	SK5,3
	C → G	283	cgCa	Arg → Arg	SK5,6‖
	C → G	127	tcCc‡§	Ser → Ser	SK6,3
GC → AT (2)	C → T	154	ggCa	Gly → Gly	SK1,6
	C → T	303	agCa	Ser → Ser	SK2,1
Other changes					
AT → GC (1)	A → G	131	aAca‡	**Asn → Ser**	SK6,3
AT → TA (5)	T → A	126**	gTact	**Tyr → Asn**	SK1,1
	T → A	134	gTm‡	**Phe → Ile**	SK1,6
	T → A	272	gTgc	**Val → Glu**	SK2,1
	A → T	292	aaAg‡	**Lys → Asn**	SK5,1
	A → T	263	tAatc‡	**Asn → Tyr**	SK8,3
CpG sites (1)	C → G	283	gCgca	**Arg → Gly**	SK5,6‖

Codons in bold type refer to hot spot codons.
*Amino acid changes are shown in bold type.
†Lesion number and region laser-captured as defined in Fig. 1*A*.
‡Base-pair substitutions occur at sites or runs on P_y-P_y/P_y either the nontranscribed or transcribed strand.
§5′G of 5′-GG-3′ on either the nontranscribed or transcribed strand.
¶Base changes potentially attributable to UVA indirectly through the production of ROS, not used as UVA fingerprints for data analysis.
‖Heterozygous sample.
**Same mutation present in underlying basal layer.

Table 2. Types of mutations detected in exons 5–9 p53 in the stratum basale of human SK

Base change (total no.)	Coding strand	Codon p53	Sequence	AA change*	Lesion/ region†
UVA fingerprints					
AT → CG (4)	T → G	257	cTgg‡	**Leu → Arg**	SK3,2
	T → G	237	aTgt	**Met → Arg**	SK4,7
	A → C	258	gaAg‡	**Glu → Asp**	SK3,2
	A → C	313	Agct‡	**Ser → Arg**	SK7,2
UVB fingerprints (0)					
GC → AT					
ROS§					
GC → TA (7)	G → T	**248**	cGga‡¶	**Arg → Leu**	SK4,4
	G → T	298	gaGc‡	**Glu → Asp**	SK5,4
	G → T	308	ctGc	**Leu → Arg**	SK6,2
	C → A	299	gCtgc‡	**Leu → Met**	SK5,4‖
	C → A	131	aaCa	**Asn → Lys**	SK8,2
	C → A	309	gCcca‡	**Pro → Thr**	SK8,4
	C → A	314	tcCt‡¶	Ser → Ser	SK8,4
GC → CG (2)	G → C	245	gGca‡	**Gly → Ala**	SK3,7
	G → C	313	aGct‡	**Ser → Thr**	SK6,2
GC → AT (1)	G → A	129	tGcc	**Ala → Thr**	SK1,4
Other changes					
AT → GC (1)	A → G	298	gAgc‡	Glu → Gly	SK5,4
AT → TA (4)	T → A	126**	gTact	**Tyr → Asn**	SK1,7
	T → A	299	cTgc‡	**Leu → Gln**	SK5,4‖
	A → T	310	aAca‡	**Asn → Ile**	SK6,2
	A → T	311	cAaca‡	**Asn → Tyr**	SK7,2
CpG sites (1)	C → A	244	ggCg	Gly → Gly	SK4,7

Codons in bold type refer to hot-spot codons.
*Amino acid changes are shown in bold type.
†Lesion number and region laser-captured as defined in Fig. 1*A*.
‡Base-pair substitutions occur at sites or runs on P_y-P_y/P_y either nontranscribed or transcribed strand.
§Base changes potentially attributable to UVA indirectly through the production of ROS, not used as UVA fingerprints for data analysis.
¶5′G of 5′-GG-3′ on either nontranscribed or transcribed strand.
‖Heterozygous sample.
**Same mutation present in overlying stratum granulosum.

stratum granulosum and two were in the basal layer. Thus, 100% of G:C → A:T transitions in SK were in the upper layers as compared with 82% in SCCs (Fig. 1*B*). Of the 18 transitions, 15 occurred at the 3′-Py of a Py-Py or Py run. Intriguingly, the only two basally located G:C → A:T transitions attributable to UVB in SCCs were also located at the 5′G of 5′-GG-3′ on the opposite strand, a hot-spot motif for UVA-induced mutagenesis by means of type 1 mechanisms (22). Four transitions at Py-Py sites (one at C → T and three at G → A), including one G → A change at the hot-spot codon 245, were detectable in dermal nonkeratinocyte stromal cells sampled from the SCCs, which otherwise may have been attributed to the keratinocytes in homogenized skin had LCM not been used (data not shown).

UVA Fingerprints (A:T → C:G Transversions) in Human SCCs and SK Show Bias Toward the Basal Epidermal Layer and Dermis. A total of 14 A:T → C:G transversions were detected in the keratinocytes. In SK, three were in the stratum granulosum and four were in the basal layer, and in SCCs, one was in the stratum granulosum and six were in the basal layer. Thus, 57% and 86% of A:T → C:G transversions were found in the basal layers of SK and SCCs (Fig. 1*C*). In contrast to the nine silent G:C → A:T transitions at Py-Py sites, all the A:T → C:G transversions lead to a base substitution. The basal layer of both SK and SCCs harbored more UVA fingerprints than UVB fingerprints (four versus zero and six versus two, respectively). Of the 14 transversions in keratinocytes, 50% (7 of 14) occurred at the 3′T of CT sequences; four of 14 were at either the 3′ or 5′T of TT sequences, three of which were flanked by cytosine residues, 5′-CT TC-3″, and the fourth was flanked by guanine residues at 5″-GTTG-3′. Seven A:T → C:G transversions were detected in the stromal cells showing a similar predilection for Py-Py sites, with two at 5′T of TT (5′GTTG 3′ and 5′CTTC3′), two at 3′T of CT sequences, and one at the 5′T of TC.

To describe the obvious histological stratification of UV band-specific damage statistically, mutations were divided into two groups (depth ≤0.4 mm or depth >0.4 mm), and a χ^2 test was performed. In the SCC group, 85% of UVA mutations had a depth ≥0.4 mm, whereas only 15% of UVB mutations were >0.45 mm deep. This difference was statistically significant ($P < 0.001$).

Most Mutations Potentially Attributable to UVA-Induced Photodamage Occur at Py-Py Sites. We initially grouped G:C → T:A and G:C → C:G transversions plus non-Py-Py G:C → A:T transitions. In SK, there was no obvious stratification between the epidermal layers when these base changes were totaled, the stratum granulosum and basal layer each harboring a total of 8 and 10, but in SCCs the basal layer harbored 19 compared with 13 in the

Table 3. Types of mutations detected in exons 5–9 p53 in the stratum granulosum of human SCC

Base change (total no.)	Coding strand	Codon p53	Sequence	AA change*	Lesion/ region†
UVA fingerprints					
AT → CG (1)	A → C	311	caAca‡	**Asn → Thr**	SCC4,1
UVB fingerprints	C → T	289	ctCc‡	Leu → Leu	SCC1,1
GC → AT (9)	C → T	157	gtCc‡	Val → Val	SCC1,6
	C → T	233	cCact‡§	**His → Tyr**	SCC1,3
	C → T	318	cCaa‡§	**Pro → Leu**	SCC4,1
	C → T	314	tCct‡	**Ser → Phe**	SCC4,3
	C → T	296	tCacc‡	**His → Tyr**	SCC4,6
	C → T	251	atCc‡	Ile → Ile	SCC7,1
	G → A	197	aGtgg‡	**Val → Met**	SCC3,1
	G → A	226	gGct‡	**Gly → Asp**	SCC6,6
ROS¶					
GC → TA (6)	G → T	290	cGca	**Arg → Leu**	SCC4,6
	C → A	195	atCc‡	Ile → Ile	SCC3,1
	C → A	208	gaCa	**Asp → Glu**	SCC3,1
	C → A	312	acCa‡§	Thr → Thr	SCC4,1
	C → A	309	cCca‡§	**Pro → His**	SCC4,3
	C → A	313	agCt‡	**Ser → Arg**	SCC4,3
GC → CG (6)	G → C	271	tGagg‡	**Glu → Gln**	SCC1,3
	G → C	228	tGact‡	**Asp → His**	SCC6,6
	G → C	326	aGaat‡	**Glu → Gln**	SCC6,6
	C → G	190	cCtc‡§	**Pro → Arg**	SCC1,1
	C → G	252	cCtca‡§	**Leu → Val**	SCC7,1
	C → G	301	gCccc‡	**Pro → Ala**	SCC1,3
GC → AT (1)	C → T	310	aaCa	Asn → Asn	SCC4,1
Other changes					
AT → GC (3)	T → C	195	aTcc‡	**Ile → Thr**	SCC1,1
	A → G	**196**	cgAg‡	Arg → Arg	SCC3,1
	A → G	**249**	gAggc‡	Arg → Gly	SCC1,1
AT → TA (3)	T → A	134	gTttt‡	**Phe → Ile**	SCC1,6
	A → T	195	tAtcc	**Ile → Phe**	SCC1,1
	A → T	310	aAca‡	**Asn → Ile**	SCC4.3
CpG sites (2)	C → T	**152**	cCgc‡§	**Pro → Leu**	SCC1,6
	C → T	158	cCgcg‡§	**Arg → Cys**	SCC1,6

Codons in bold type refer to hot-spot codons.
*Amino acid changes are shown in bold type.
†Lesion number and region laser-captured as defined in Fig. 1*A*.
‡Base-pair substitutions occur at Py-Py sites or Py runs on either nontranscribed or transcribed strand.
§5′G of 5′-GG-3′ on either nontranscribed or transcribed strand.
¶Base changes potentially attributable to UVA indirectly through the production of ROS, not used as UVA fingerprints for data analysis.

Table 4. Types of mutations detected in exons 5–9 p53 in the stratum basale of human SCC

Base change (total no.)	Coding strand	Codon p53	Sequence	AA change*	Lesion/ region†
UVA fingerprints					
AT → CG (6)	T → G	238	tgTa	**Cys → Trp**	SCC1,2
	T → G	257	cTgg‡	**Leu → Arg**	SCC6,7
	T → G	220	cTatg‡	**Tyr → Asp**	SCC8,2
	T → G	203	gTgg	**Val → Gly**	SCC8,4
	A → C	320	Aaga‡	**Lys → Gln**	SCC4,2
	A → C	331	cAgg‡	**Gln → Pro**	SCC5,2
UVB fingerprints (2)	C → T	315	cCtc‡§	**Ser → Phe**	SCC7,2
GC → AT	G → A	293	aGggg‡§	**Gly → Arg**	SCC4,4
ROS¶					
GC → TA (10)	G → T	305	aaGc‡	**Lys → Asn**	SCC2,4
	G → T	283	cGcca	**Arg → Leu**	SCC3,4
	G → T	317	caGc	**Gln → His**	SCC4,2
	C → A	309	cCca‡§	**Pro → His**	SCC1,4
	C → A	289	tCtcc‡	**Leu → Met**	SCC2,4
	C → A	314	tCct‡	**Ser → Tyr**	SCC4,2
	C → A	316	ccCc‡§	Pro → Pro	SCC4,2
	C → A	228	gaCt‡	**Asp → Glu**	SCC6,2
	C → A	289	ctCc‡	Leu → Leu	SCC4,4
	C → A	308	aCtgc‡	**Leu → Met**	SCC6,4
GC → CG (6)	G → C	215	aGtg‡	**Ser → Thr**	SCC1,2
	G → C	317	caGc‡	**Gln → His**	SCC6,4
	G → C	325	tgGa‡	**Gly → Ala**	SCC7,2
	C → G	228	gaCt‡	**Asp → Glu**	SCC2,4
	C → G	219	ccCt‡§	Pro → Pro	SCC8,2
	C → G	310	aaCa	**Asn → Lys**	SCC6,4
GC → AT (3)	C → T	310	aaCa	Asn → Asn	SCC1,4
	C → T	**245**	ggCa	Gly → Gly	SCC6,2
	C → T	242	tgCa	Cys → Cys	SCC6,7
Other changes					
AT → GC (3)	A → G	307	gcAc	Ala → Ala	SCC1,4
	A → G	204	gAgt‡	**Glu → Gly**	SCC8,4
	T → C	315	cTctc‡	**Ser → Pro**	SCC5,2
AT → TA (7)	T → A	274	gtTt‡	Val → Val	SCC5,4
	T → A	278	ccTg‡	Pro → Pro	SCC4,4
	A → T	266	ggAc‡	Gly → Gly	SCC2,4
	A → T	280	gAgag*	**Arg → stop**	SCC3,4
	A → T	281	gAcc*	**Asp → Val**	SCC3,4
	A → T	311	cAaca*	**Asn → Tyr**	SCC7,2
	A → T	211	cActt	**Thr → Ser**	SCC8,2

Codons in bold type refer to hot-spot codons.
*Amino acid changes are shown in bold type.
†Lesion number and region laser-captured as defined in Fig. 1*A*.
‡Base-pair substitutions occur at sites or runs on Py-Py/Py either nontranscribed or transcribed strand.
§ 5′G of 5′-GG-3′ on either nontranscribed or transcribed strand.
¶Base changes potentially attributable to UVA indirectly through the production of ROS, not used as UVA fingerprints for data analysis.

stratum granulosum. When considered individually, there was stratification for the G:C → T:A transversions, with the bias toward the basal layer in both SK and SCCs, the stratum granulosum of SK harboring one (versus seven in the basal layer) and SCCs harboring six (versus 10 in the basal layer). In total, in the keratinocytes there were 24 G:C → T:A transversions: 7 G → T and 17 C → A. Six of the G → Ts were basal, three occurring at Py-Py sites on the opposite strand and one at the hot-spot codon 248 (contains a CpG), with the mutated base at 5′G of 5′-CpGG-3′, and six of seven G → Ts including the one in the stratum granulosum occurred at 5′-GC-3′. Of the 17 C → As, 11 were in the basal layer (four in SK and seven in SCCs) versus 6 in the stratum granulosum (one in SK and five in SCCs), with 15 of 17 occurring at Py-Py sites all on the nontranscribed strand. G:C → C:G transversions, on the other hand, showed no strand bias and no basal layer bias in the SCCs. In SK there were five in the stratum granulosum and two in the basal layer. Again, 17 of the 19 G:C → C:G transversions were at Py-Py sites.

In the keratinocytes there were seven non-Py-Py G:C → A:T transitions. We also detected G:C → T:A, G:C → C:G, and non-Py-Py G:C → A:T base changes in stromal cells from both SCCs and SK, with 73.6% (14 of 19) occurring at Py-Py/Py runs on either strand.

A:T → G:C Transitions Constitute a Minority of Base Changes in SK and SCCs and Together with A:T → T:A Transversions Occur Mostly at Py-Py Sites. There were six A:T → G:C transitions in SCCs (four A → G and two T → C), three in the basal and three in the granular keratinocytes; five of the six occurred at Py-Py sites. There were two A:T → G:C transitions in SK (two A → G) at Py-Py/Py runs on the transcribed strand: 5′-CTC-3′ (codon 298) and 5′-GTT-3′(codon 131). The 19 A:T → T:A transversions showed no

MEDICAL SCIENCES

particular strand or epidermal layer bias (8 T → A versus 11 A → T), with 8 in the granular layer and 11 in the basal layer; 14 occurred at Py-Py/Py runs. Of the 19 A:T → T:A transversions, 10 were at GT-(Py/Purine), 2 were at 5′-CTG-3′, 4 were at 3′ TT/C, and 2 were at 5′-T TT-3′ on either strand and codon 195 at 5′-TAT-3′.

The Four G:C → A:T Transitions at CCpG Sites Were Not Located in the Basal Epidermal Layer. The four transitions at CpG islands occurred at the motif 5′-CCpG-3′; two were located in the stratum granulosum and two were located in the dermal, nonkeratinocytes, one of which was a G → A change at hot-spot codon 282 at a CpG on the transcribed strand. In each case the mutant base was a CC potentially attributable to the 5′G of 5′-GG-3′ on the opposing strand.

Dermal Inflammation Does Not Influence Mutational Results. To exclude endogenous ROS production as a confounder in our ability to attribute base changes to the effects of UVA, one of the rete pegs (Fig. 1*A*, region 4) selected was always adjacent to a dense inflammatory infiltrate and stromal cells sampled (Fig. 1*A*, region 5). Characterization of the stroma showed a principally neutrophilic infiltrate with a mean neutrophil count of 462 cells per mm^2 in SK compared with 424 cells per mm^2 in SCCs. In contrast, few macrophages were identified in this region (mean: 19 cells per mm^2 in SK and 50 cells per mm^2 in SCCs). A significant proportion of stromal cells was positive for hydrogen peroxide production, suggesting endogenous ROS production (796 cells per mm^2 in SK and 278 cells per mm^2 in SCCs). No correlation was found between either neutrophil numbers or the number of hydrogen peroxide-positive cell levels and the number of ROS-associated mutations in overlying keratinocytes. No difference was observed when comparing UVA mutation numbers in the areas adjacent to inflammation with the areas that were not adjacent to inflammation.

IHC Detection of 8-oxoG and p53 Showed Basal Localization in the Epidermis, Whereas CPD Staining Was Predominantly Superficial. Immunohistochemical analysis provides a snapshot of unrepaired damage induced by recent exposure to both UVA and UVB radiation. Antibody staining of CPD (a UVB marker) showed suprabasal localization in the epidermis (Fig. 1*D*), whereas 8-oxoG staining (detecting UVA damage) was predominantly basal (Fig. 1*E*). For each antibody the difference in the number of immunoreactive cells in the basal versus the superficial epithelial layers was statistically significant ($P < 0.05$). Normal sun-exposed skin from age-matched controls showed minimal antibody staining, whereas non-sun-exposed skin was negative in all samples. Controls without primary antibody were also negative in all samples. p53-positive cells were detected throughout the epidermis of both SK and SCCs but not in normal skin. There were more p53-positive cells in the basal compared with the suprabasal layers (Fig. 1*F*).

Discussion

In this study, we sought to examine the role of UVA radiation in skin carcinogenesis by looking for evidence of UVA fingerprint mutations in a range of lesions involved in the progression to SCC of the skin in humans. Using LCM for mutational profile mapping, we demonstrate a major role for UVA in the vital stem cell region of the epidermis during the process of skin malignant transformation.

The finding in this study of UVA fingerprint mutations in skin cancer is an important one. The failure of previous studies to detect UVA fingerprint mutations (23) reflects the importance of using highly sensitive techniques such as LCM in heterogeneous tissue such as skin along with purposeful examination of the basal epithelial layer. Using the methods outlined, we were able to sequence p53 exons 5–9 in 100% of microdissected samples successfully. Our approach was sufficiently sensitive to detect at least one p53 mutation in all SCCs and SK, when lower values had been reported (7, 24). Many studies focus DNA analysis to codons frequently mutated by UVB, called hot spots. Our PCR amplification and sequencing did not have this restriction. Thus, in addition to two G:C → A:T transitions at hot spots 278 and 152 in the stratum granulosum, we found a broader spectrum and higher frequency of mutations than is usually reported. UVA and UVB fingerprint mutations were detected in both SK and SCCs in nearly equal numbers and showed a striking spatial distribution, with UVA fingerprints largely basally distributed as opposed to a suprabasal predominance of UVB mutations.

The location of DNA photolesions within the epidermis is potentially critical in assigning relative significance of each particular bandwidth to the process of tumor formation. Basally located stem cells give rise to skin tumors (25), and therefore mutations at this location are likely to be important in skin carcinogenesis. The distinctive localization of mutations demonstrated in our mapping is consistent with conventional knowledge on the depth of UVA and UVB penetration (2). The penetration of shorter-wavelength UVB radiation is predominantly confined to the superficial epidermis. This is consistent with our finding that the majority of UVB mutations in SCCs and SK were localized to the upper epithelial layers. The identification of UVA mutations in basal layers corresponds to the greater ability of UVA compared with UVB to penetrate down to the basal epithelial layers and dermis. That fewer UVA fingerprint mutations were identified in the superficial epidermal layers (where one would expect the greatest UVA load) might reflect a decreased sensitivity of upper-differentiating keratinocytes to the effects of UVA compared with basal cells or differences in the repair capacities of cells. Basal and suprabasal distributions of p53 staining have been detected previously after irradiation with UVA or UVB, respectively (26), consistent with our observation that p53 staining colocalized with UVA mutations in the basal and UVB mutations in the suprabasal layers. It is unknown why there were more p53-positive cells in the basal than the suprabasal layer. The layers may respond differently to DNA damage, or UVA may stabilize p53 more effectively than UVB. Thus, the basal localization of both p53 IHC staining and UVA fingerprint mutations noted in both SK and SCCs in this study suggests that UVA in sunlight is likely to be important for human skin carcinogenesis.

The predominance of C → T (15 of 18) versus G → A (3 of 18) reflects the well characterized bias toward repair of UVB-induced photoproducts from the transcribed strand of p53 (27). No such strand bias was evident in UVA mutations, which were distributed evenly between the strands (six A → C and eight T → G). Given the obvious bias seen with the UVB-induced fingerprint mutations, the finding with the UVA fingerprints, present at nearly equal numbers, is unlikely to represent an artifact because of the relatively small numbers of tumors/mutations examined. Rather, it may represent as-yet-unknown differences in the types of photoproducts induced and repaired between the two wavebands. The three T → G transversions, at non-Py-Py sites detected on the coding strand at 5′GTG3′, 5′GTA3′, and 5′ATG3′ in the keratinocytes and the 5′ATG3′ in the stromal cells, indicate that an as-yet-unknown nondimer UVA-induced photolesion plays some role in the induction of a subset of A:T → C:G transversions and is in accord with *in vitro* findings showing that not all UVA-induced transversions occur at Py-Py sites (8).

The identification of UVA mutations in both SCCs and premalignant SK in almost identical proportions implicates an early role for this band of radiation in tumor progression. Importantly, analysis of the IARC TP53 Mutation Database

(www-p53.iarc.fr) shows that a small number of A:T → C:G changes have been detected and comprise 0.96% (1 of 104) of mutations detected in SK and 6.09% (12 of 197) of mutations detectable in skin SCCs. The relative underrepresentation of UVA-induced changes reported in the literature most likely reflects biases associated with p53 reporting, study design, and detection methods (28). That A:T → C:G transversions are found in SK and SCCs supports the conclusion that these base changes previously induced by UVA in mutagenesis model systems are attributable to the UVA fraction of solar light and that they play a role in human skin carcinogenesis.

To evaluate fully the extent and pattern of acute UVA and UVB damage, IHC was performed on the same samples on which mutational analyses had been performed and confirmed the pattern of UV damage noted. The anti-thymidine dimer antibody is principally a marker of UVB damage (18). Our finding of CPD staining throughout the epidermis (but maximal staining in the upper layers) is consistent with the more superficial penetrative capacity of UVB radiation and confirms the pattern of UVB fingerprint mutations noted. Such predominantly superficial epidermal staining of CPD has been described previously after UVB radiation at 290 nm (29). 8-oxoG is a commonly used marker of UVA oxidative damage (30) and can lead to G → T transversions (31). We found a striking bias in the basal location of 8-oxoG staining in all SK and SCCs detected with IHC, and it correlated with the more basal epithelial distribution of G:C → T:A transversions, along with a basal predominance of UVA fingerprint mutations. Several lines of evidence have shown the relationship between UV exposure and the production of free radicals, particularly superoxide ions, singlet oxygen, hydrogen peroxide, and hydroxyl radicals (6, 32, 33). Given the ubiquitous nature of ROS, it is generally not possible to ascribe a particular base change to the action of any particular endogenously or exogenously produced ROS (34). This said, there was no correlation between the detection of G:C → T:A, G:C → C:G, and G:C → A:T base changes (either considered in total or individually) in the overlying basal keratinocytes and the presence of dermal inflammation, which suggests that at least some of these base changes may have been the result of exogenously (UVR-induced) rather than endogenously generated mutagenic events. Of the 24 G:C → T:A transversions (7 G → T and 17 C → A) that we found in the keratinocytes, the C → As are extremely interesting because most (15 of 17) occurred at Py-Py sites, all on the nontranscribed strand, five of which were at the 5′G of 5′-GG-3′ or in a guanine run on the opposite strand [codons 309 (on two), 312, 314, and 316, and three of seven G → Ts occurred at Py-Py sites (one at the 5′G of 5′-GG-3′)]. This result suggests that they are UV-induced rather than induced by endogenously generated ROS and that CPDs not 8-oxoG may have been the premutagenic lesion.

Our finding that p53 mutations are not identical in microdissected samples from different regions of the same lesion is consistent with studies showing cytogenetically unrelated clones in a large fraction of SCCs and SK (35, 36). In 107 metaphase cells analyzed from a single SK, 32 were normal, 19 had nonclonal aberrations, and the remaining 56 abnormal cells gave rise to eight cytogenetically unrelated clones (35). Likewise, skin SCCs have tremendous cytogenetic heterogeneity, varied degrees of karyotypic complexity, and obvious polyclonality (37). During skin cancer development, before the formation of a clinically detectable lesion, clonal expansion of an initiated mutant cell is presumably required to create a target large enough for one of the progeny to acquire the next mutation, which gives it a growth advantage (38, 39). The results of our studies, using LCM and nonselective PCR, are consistent with these observations that subsequent mutations in individual cells of mutated clones result in the clinical lesion becoming a heterogeneous mix of mutated clones. Our study further shows that these heterogeneous clones are present in distinct spatial regions of the tumor.

In conclusion, we have demonstrated that UVA fingerprint mutations are detectable in transformed keratinocytes from human skin SCCs and SK. Using LCM and immunohistochemical staining, we identified a distinct spatial distribution of UVA and UVB mutational damage, underscoring known penetrance capacities of each waveband. It may be that the widespread use of UVB-blocking sunscreens in Australia, as predicted (8), has led to an increase in human exposure to UVA and allowed us to detect these changes now. The predominance of UVA mutations in the basal cell layer reinforces the pivotal role UVA may play in the malignant transformation of human skin. The importance of protecting the population not just from UVB but also from UVA irradiation has profound implications on public health worldwide.

1. Setlow, R. (1974) *Proc. Natl. Acad. Sci. USA* **71,** 3363–3366.
2. Bruls, W. A., Slaper, H., van der Leun, J. C. & Berrens, L. (1984) *Photochem. Photobiol.* **40,** 485–494.
3. Mukhtar, H., Forbes, P. D. & Ananthaswamy, H. N. (1999) *Photodermatol. Photoimmunol. Photomed.* **15,** 91–95.
4. De Gruijl, F. R., Sterenborg, H. J., Forbes, P. D., Davies, R. E., Cole, C., Kelfkens, G., van Weelden, H., Slaper, H. & van der Leun, J. C. (1993) *Cancer Res.* **53,** 53–60.
5. Sterenborg, H. J. & van der Leun, J. C. (1990) *Photochem. Photobiol.* **51,** 325–330.
6. Runger, T. M. (1999) *Photodermatol. Photoimmunol. Photomed.* **15,** 212–216.
7. Brash, D. E., Rudolph, J. A., Simon, J. A., Lin, A., McKenna, G. J., Baden, H. P., Halperin, A. J. & Ponten, J. (1991) *Proc. Natl. Acad. Sci. USA* **88,** 10124–10128.
8. Drobetsky, E. A., Turcotte, J. & Chateauneuf, A. (1995) *Proc. Natl. Acad. Sci. USA* **92,** 2350–2354.
9. Robert, C., Muel, B., Benoit, A., Dubertret, L., Sarasin, A. & Stary, A. (1996) *J. Invest. Dermatol.* **106,** 721–728.
10. Harris, C. C. (1993) *Science* **262,** 1980–1981.
11. Persson, A. E., Ling, G., Williams, C., Backvall, H., Ponten, J., Ponten, F. & Lundeberg, J. (2000) *Anal. Biochem.* **287,** 25–31.
12. Zhang, X., Rosenstein, B. S., Wang, Y., Lebwohl, M., Mitchell, D. M. & Wei, H. (1997) *Photochem. Photobiol.* **65,** 119–124.
13. Agar, N. S., Halliday, G. M., Barnetson, R. S. & Jones, A. M. (2003) *J. Cutan. Pathol.* **30,** 265–270.
14. Schifter, M., Jones, A. M. & Walker, D. M. (1998) *J. Oral Pathol. Med.* **27,** 318–324.
15. Kawanishi, S., Hiraku, Y. & Oikawa, S. (2001) *Mutat. Res.* **488,** 65–76.
16. Lee, D. H. & Pfeifer, G. P. (2003) *J. Biol. Chem.* **278,** 10314–10321.
17. Berhane, T., Halliday, G. M., Cooke, B. & Barnetson, R. S. (2002) *Br. J. Dermatol.* **146,** 810–815.
18. Roza, L., van der Wulp, K. J., MacFarlane, S. J., Lohman, P. H. & Baan, R. A. (1988) *Photochem. Photobiol.* **48,** 627–633.
19. Yarborough, A., Zhang, Y. J., Hsu, T. M. & Santella, R. M. (1996) *Cancer Res.* **56,** 683–688.
20. Vojtesek, B., Bartek, J., Midgley, C. A. & Lane, D. P. (1992) *J. Immunol. Methods* **151,** 237–244.
21. Dannenberg, A. M., Jr., Schofield, B. H., Rao, J. B., Dinh, T. T., Lee, K., Boulay, M., Abe, Y., Tsuruta, J. & Steinbeck, M. J. (1994) *J. Leukocyte Biol.* **56,** 436–443.
22. Ito, K., Inoue, S., Yamamoto, K. & Kawanishi, S. (1993) *J. Biol. Chem.* **268,** 13221–13227.
23. van Kranen, H. J., de Laat, A., van de Ven, J., Wester, P. W., de Vries, A., Berg, R. J., van Kreijl, C. F. & de Gruijl, F. R. (1997) *Cancer Res.* **57,** 1238–1240.
24. Campbell, C., Quinn, A. G., Ro, Y. S, Angus, B. & Rees, J. L. (1993) *J. Invest. Dermatol.* **100,** 746–748.
25. Morris, R. J. (2000) *J. Clin. Invest.* **106,** 3–8.
26. Campbell, C., Quinn, A. G., Angus, B., Farr, P. M. & Rees, J. L. (1993) *Cancer Res.* **53,** 2697–2699.
27. Dumaz, N., Drougard, C., Sarasin, A. & Daya-Grosjean, L. (1993) *Proc. Natl. Acad. Sci. USA* **90,** 10529–10533.
28. Hernandez-Boussard, T., Montesano, R. & Hainaut, P. (1999) *Genet. Anal.* **14,** 229–233.
29. Young, A. R., Chadwick, C. A., Harrison, G. I., Nikaido, O., Ramsden, J. & Potten, C. S. (1998) *J. Invest. Dermatol.* **111,** 982–988.
30. Douki, T., Perdiz, D., Grof, P., Kuluncsics, Z., Moustacchi, E., Cadet, J. & Sage, E. (1999) *Photochem. Photobiol.* **70,** 184–190.
31. Cheng, K. C., Cahil, D. S., Kasai, H., Nishimura, S. & Loeb, L. A. (1992) *J. Biol. Chem.* **267,** 166–172.
32. Kielbassa, C., Roza, L. & Epe, B. (1997) *Carcinogenesis* **18,** 811–816.
33. Roza, L., van der Schans, G. P. & Lohman, P. H. (1985) *Mutat. Res.* **146,** 89–98.
34. Kamiya, H. (2003) *Nucleic Acids Res.* **31,** 517–531.
35. Jin, Y., Jin, C., Salemark, L., Wennerberg, J., Persson, B. & Jonsson, N. (2002) *Cancer Genet. Cytogenet.* **136,** 48–52.
36. Heim, S., Jin, Y., Mandahl, N., Biorklund, A., Wennerberg, J., Jonsson, N. & Mitelman, F. (1988) *Cancer Genet. Cytogenet.* **36,** 149–153.
37. Jin, Y., Martins, C., Jin, C., Salemark, L., Jonsson, N., Persson, B., Roque, L., Fonseca, I. & Wennerberg, J. (1999) *Genes Chromosomes Cancer* **26,** 295–303.
38. Jonason, A. S., Kunala, S., Price, G. J., Restifo, R. J., Spinelli, H. M., Persing, J. A., Leffell, D. J., Tarone, R. E. & Brash, D. E. (1996) *Proc. Natl. Acad. Sci. USA* **93,** 14025–14029.
39. Zhang, W. G., Remenyik, E., Zelterman, D., Brash, D. E. & Wikonkal, N. M. (2001) *Proc. Natl. Acad. Sci. USA* **98,** 13948–13953.